Chaos in wavelength with a feedback tunable laser diode

Jean-Pierre Goedgebuer*, Laurent Larger*, and Henri Porte*
GTL-CNRS Telecom, UMR 6603, Georgia Tech Lorraine, 2-3 rue Marconi, 57070 Metz, France

Franck Delorme
France Telecom, CNET, Boîte Postale 107, 92225 Bagneux Cedex, France
(Received 14 August 1997; revised manuscript received 17 November 1997)

Wavelength is used to induce optical nonlinearities and to generate chaos from a multielectrode wavelength tunable laser diode. Chaotic modulation of wavelength ruled by a nonlinear differential difference equation is demonstrated. The method offers a high flexibility, which should open the way to simple chaotic systems with complicated nonlinear functions. [S1063-651X(98)06003-6]

PACS number(s): 05.45+b, 42.65.Sf, 42.55.Px

I. INTRODUCTION

There are many situations, in many disciplines, that can be described by a first order, nonlinear differential difference equation (also termed Ikeda's equation), which may be expressed in the normalized form

$$X(t)+\frac{dX(t)}{dt}=\beta F[X(t-t_R)] \tag{1}$$

in which the function $F[X]=\sin^2[X(t-t_R)]$ is a periodic function of a variable X evaluated at a retardation time t_R, and β is the bifurcation parameter. Such equations exhibit an array of dynamical behavior, from stable points to a bifurcating hierarchy of stable cycles and to chaotic fluctuations. They are well known to occur in optical or electrical bistable systems (whose nonlinearity is the F function) with a delayed feedback. In this work, we begin by noting that the chaotic regimes reported in optics concern systems in which the optical turbulence is characterized by a chaotic variation of light intensity [1–5] or polarization [6]. Chaotic fluctuations of wavelength were also reported, especially from semiconductor lasers. However, they are closely coupled to chaos in intensity, which makes their handling complex [7]. On the other hand, the experimental regimes that obey Eq. (1) reported so far concern mainly systems with low bifurcation parameters ($\beta<3$), yielding simple chaotic processes, while theoretically $\beta>15$ is needed to have a chaotic process with a Gaussian probability density law [8]. This feature, combined with a high dimensional chaos, is required to improve confidentiality in cryptography by chaos, for instance.

The object of this paper is to show that wavelength-induced nonlinearities can be used advantageously to generate chaos. Such nonlinearities were proposed originally for exotic demonstrations of bistability in wavelength [9]. The recent advances in the wavelength agility of tunable multisection laser diodes make them very attractive to implement simple generators of chaos with very complex dynamics. Several other experimental devices have been extensively studied for their chaotic dynamics, such as He-Ne lasers with electro-optic feedback [10], Q-switched and mode-locked NO_2 and CO_2 lasers with intracavity absorbers [11], pulsed Nd-YAG lasers with modulation of the cavity loss [12], etc. but their chaotic dynamics is obtained in intensity or in polarization. Most of them are more complicated than that reported here, and do not feature a high applicability as ''tunable'' generators of chaos in terms of systems. They are characterized by nonlinearities that are intrinsic to the laser itself, without offering a variety of possibilities in changing the type of nonlinearity, and hence of dynamics. In contrast, the method reported in the following is general and can be applied to a variety of chaos problems. Physically, it is essentially due to the use of wavelength to generate nonlinearities, instead of intensity.

II. EXPERIMENTAL CONFIGURATION AND MODELING

Let us consider the wavelength tunable two-electrode semiconductor laser with the feedback loop, as illustrated in Fig. 1. In a two-electrode laser diode, the wavelength is fixed at a given value Λ_0 by adjusting a couple of bias currents (I_0,I_1) on each of the electrodes, and can be tuned electrically around Λ_0 by varying current I_0 by i, while keeping I_1 constant. The power emitted is wavelength independent. In

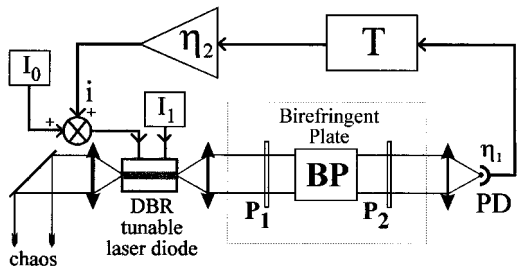

FIG. 1. Generator of chaos in wavelength using a wavelength tunable laser diode with a nonlinear feedback loop. The nonlinearity is induced by the birefringent plate BP set between two crossed or parallel polarizers P_1 and P_2. The intensity detected by the photodetector PD is a nonlinear function of the wavelength emitted by the laser diode. η_1 is the gain of the photodetector and T the time delay introduced in the feedback loop.

*Permanent address: Laboratoire d'Optique P.M. Duffieux, UMR CNRS 6603, Université de Franche-Comté, 25030 Besançon Cedex, France.

the conditions of continuous wavelength tuning i.e., without mode hopping, the wavelength shift λ is proportional to the variation i of the injection current, $\lambda(t)=\alpha i(t)$, where $\alpha=d\Lambda/di$ is the tuning rate of the laser diode, and the emitted wavelength is $\Lambda(t)=\Lambda_0+\lambda(t)$. The feedback loop consists of a birefringent plate (BP) whose fast and slow axes are at 45° to two crossed polarizers P_1 and P_2, a photodetector (PD) with a time response τ, a delay line with a retardation time T, and a voltage-to-current converter. The latter provides the tuning current i, which is superimposed to the bias current I_0. The plate BP induces the nonlinear function F between the wavelength emitted by the laser diode and the optical power detected by the photodetector, through its spectral transmission curve, which is that of a so-called ''channeled spectrum'' $F(\Lambda)=\sin^2(\pi D/\Lambda)$, where D is the optical path difference (OPD) of BP. Since $\lambda(t)\ll\Lambda_0$, F can be developed around the center wavelength Λ_0 as

$$F(\lambda)=\sin^2\left(\frac{\pi D\lambda}{\Lambda_0^2}-\phi_0\right), \tag{2}$$

with $\phi_0=\pi D/\Lambda_0$. The F function is a $\sin^2$ function, which exhibits oscillations spaced in wavelength by a free spectral range (FSR)$\approx\Lambda_0^2/D$. The photodetector converts linearly the detected power $F(\lambda)$ in a feedback voltage with a gain η_1, which is then converted by a voltage-to-current converter in the feedback current $i(t)$ with a conversion efficiency η_2. The response times of the electronic devices in the feedback loop and of the laser diode are much smaller than that, τ, of the photodetector, which behaves as a low pass filter with derivative properties. Taking the dynamical properties of the device into consideration, the modulation of wavelength $\lambda(t)$ is shown to be ruled by the following differential difference equation:

$$\lambda(t)+\tau\frac{d}{dt}\lambda(t)=\beta_\lambda\sin^2\left[\frac{\pi D}{\Lambda_0^2}\lambda(t-T)-\phi_0\right], \tag{3}$$

where $\beta_\lambda=P_0\alpha\eta_1\eta_2$ is the bifurcation parameter (expressed in wavelength units), and P_0 is the optical power of the laser diode. Note that Eq. (3) can be expressed in the normalized form of Eq. (1) with $X(t)=\pi D\lambda(t)/\Lambda_0^2$, $\beta=\pi D\beta_\lambda/\Lambda_0^2$, and $t_R=T/\tau$. For $T\gg\tau$, a convenient way to analyze the instability of the device is to neglect the differential term and to express Eq. (3) in the form:

$$\lambda_n=\beta_\lambda F[\lambda_{n-1}]=\beta_\lambda\sin^2\left(\frac{\pi D}{\Lambda_0^2}\lambda_{n-1}-\phi_0\right), \tag{4}$$

where $\lambda_n=\lambda(t_0+nT)$, n being an integer and t_0 being a certain initial time. The device is unstable [13] if the slope at the intersection points of the 45° line $\lambda_n=\lambda_{n-1}$ with the $\sin^2$ function of λ_n versus λ_{n-1} exceeds $|\pm 45°|$ i.e., if $\beta_\lambda|dF/d\lambda|>1$, as shown in Fig. 2. Then the laser wavelength fluctuates periodically or chaotically, depending on the values of β_λ, ϕ_0, and of the number of oscillations of F within the tuning range of the laser diode. Increasing the number of oscillations of F is equivalent to increasing the nonlinearity strength β in Eq. (1). Theoretical and experimental studies of the solutions of differential difference equations in which the nonlinearity is a $\sin^2$ function have been extensively treated and we refer the reader, for instance, to hybrid systems described in Refs. [2–4]. However, the experiments reported so far concern mainly systems with $\beta<3$, that may result in a lack of generality [e.g., the dimension of chaos increases linearly with β and the chaotic solutions of Eq. (1) are shown to feature a Gaussian-Markovian character for $\beta>15$ [8]]. The reason is twofold: (i) in such systems, increasing the bifurcation parameter is implemented electrically, increasing the gain in the feedback loop, that sets an upper limit due to electronics, (ii) the nonlinearity $F[X]$ in the previous systems is induced by Pockels effect or Bragg diffraction (which are well known to produce $\sin^2$ transfer curves in power) with the disadvantage that the driving voltages V are also limited due to electronics. This results in an F function truncated to a single oscillation and to low values of β, yielding simple chaotic processes.

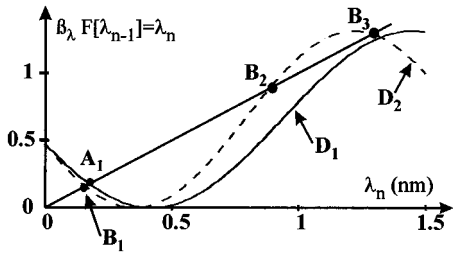

FIG. 2. Graphical representation of $\lambda_n=\beta_\lambda F[\lambda_{n-1}]$ for two values D_1 and D_2 of the optical path difference. For D_1 (solid line), a single intersection point A_1 occurs with the line $\lambda_n=\lambda_{n-1}$. For D_2 (dashed line), three intersection points B_1, B_2, B_3 occur.

The situation is different when using the present system. A high bifurcation parameter can be obtained optically as well as electrically. Periodic nonlinearities with a large number of oscillations can be easily achieved optically with large OPDs. The maximum number N_m of oscillations of F within the λ range is set by the spectral resolution of the device, i.e., the laser linewidth $d\Lambda$, and is expressed as $N_m\approx\Delta\Lambda/d\Lambda\approx D_m\Delta\Lambda/\Lambda_0^2$. It can be very high, typically 1.5×10^4 for a 10 MHz linewidth. The maximum bifurcation parameter thus obtained is

$$\beta\approx\pi N_m\approx\pi D_m\Delta\Lambda/\Lambda_0^2, \quad \text{with} \quad D_m\approx\Lambda_0^2/d\Lambda. \tag{5}$$

Here β is written in its normalized form for easy comparison. β is 5×10^4 times higher than in previous systems but there are experimental limitations with implementing the 25 m OPD thus required. Practically, $\beta=30$ seems to be a maximum when using birefringent slabs with maximum achievable OPDs, $D_m\sim15$ mm; β in the range of 10^2-10^3 are easily achievable with fiber Mach-Zehnder interferometers with OPDs up to D_m of several tens of cm.

To check the validity of the method, we made simulations of the behavior of the device. Figure 3 shows two calculated bifurcation diagrams of the laser wavelength plotted against the bifurcation parameter β_λ, for two fixed values of the OPD: $D_1=1.6$ mm and $D_2=1.9$ mm. The parameter ϕ_0 is $\phi_0=\pi/4$ in the two cases. The bifurcation parameter β_λ is varied from 0 to 1.5 nm in order to simulate wavelength tuning within the entire spectral range of the laser diode used, which was $\Delta\Lambda=1.5$ nm. The two bifurcation diagrams are calculated from the differential difference equation (3),

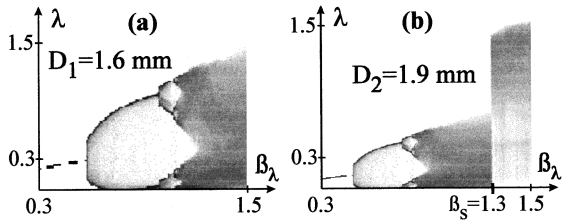

FIG. 3. Bifurcation diagrams calculated for D_1 and D_2. The axes are in nm. A sudden widening of the chaotic attractor occurs at $\beta_s = 1.3$ nm (interior crisis) in (b).

using parameter values compatible with those in the experiments discussed later. In the first case [Fig. 3(a)], D_1 is such that a single oscillation occurs within the tuning range of the laser diode, yielding a single intersection point A_1 (see Fig. 2). The bifurcation diagram is similar to that discussed, for instance, in [4]. In the second case, the F function exhibits two oscillations, yielding the intersection points B_1, B_2, B_3. The bifurcation diagram thus obtained is given in Fig. 3(b) and illustrates an interior crisis at β_s. It is formed by two scenarios. For a range of β_λ less than the critical value $\beta_s = 1.3$ nm (which also may be regarded as a switching bifurcation parameter), the chaotic attractor lies within a band, which suddenly widens when the bifurcation parameter increases past the critical value $\beta_s = 1.3$ nm. Then the bifurcation diagram maps another scenario, which denotes, for the parameter values chosen, a full chaos different from the previous one, as can be clearly seen in Fig. 3(b). A detailed discussion of such sudden changes of chaotic orbits is given in [14].

III. EXPERIMENTAL VERIFICATION

The behavior of the system was checked experimentally using a two electrode distributed Bragg reflector laser diode. The laser diode featured a tuning range $\Delta\Lambda = 1.5$ nm. One electrode was connected to the feedback loop (current I_0). The value of the center wavelength could be adjusted using a bias current I_1 on the other electrode. The linewidth was 10 MHz. The wavelength could be tuned continuously, i.e., without mode hopping, by varying current I_0 (while keeping current I_1 at a fixed value) with a tuning rate $\alpha = 0.2$ nm/mA. The power emitted by the laser diode was $P_0 = 1$ mW and was checked to be wavelength independent. The response time of the photodetector available was $\tau = 9\ \mu$s, much larger than the response times of the delay line and of the laser diode which were 100 and 10 ns, respectively. We introduced a delay $T = 0.5$ ms by inserting an analog sampled delay circuit in the feedback loop. The delay circuit was a charge-coupled device memory operating with an input signal that was sampled every 1 μs, that was negligibly small compared to the response time of the system. First, the center wavelength was adjusted at $\Lambda_0 = 1550$ nm and the retardation plate BP was an antireflection coated calcite slab of thickness $t = 10$ mm with an OPD of $D_1 = |n_e - n_0| t = 1.6$ mm where $|n_e - n_0| = 0.157$ is the calcite birefringence at 1550 nm wavelength. The value of the ϕ_0 parameter was $\pi/4 + 2m\pi$ (m is an integer). Then the system operated with the F function exhibiting a single oscillation with a single intersection point. Figure 4(a) shows the bifurcation diagram thus obtained by varying the gain η_1 of the photodetector, and hence the bifurcation parameter β_λ. The bifurcation diagram was obtained by analyzing the wavelength emitted by the laser diode through a Fabry-Pérot interferometer operating at the inflection point of an edge of its spectral transmission curve to convert linearly the modulation of wavelength λ into a detectable modulation of intensity. We observed the well-known transitions and bifurcations from the period-two oscillation to the period-four state, then to the prechaotic regime (period-two chaos), and to full chaos.

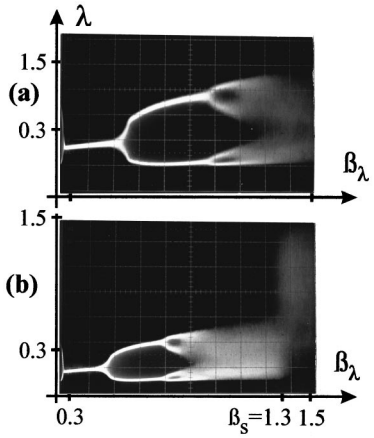

FIG. 4. Experimental bifurcation diagrams for D_1 in (a), and D_2 in (b). In (b), the interior crisis at $\beta_s = 1.3$ nm can be clearly seen.

In a second step, we used another slab with an OPD of $D_2 = 1.9$ mm, yielding an F function with two oscillations located within the tuning range of the laser diode (unfortunately, no other birefringent slab with a larger OPD was available at the laboratory when we made the experiments). The ϕ_0 parameter was kept at $\pi/4 + 2p\pi$ (p is an integer). The bifurcation diagram thus obtained is shown in Fig. 4(b). Two maps of chaos can be clearly seen. A sudden widening of the chaotic attractor occurs at the critical value $\beta_s = 1.3$ nm, in good accordance with the theoretical predictions. Finally, in order to check which part of the F function operated for values of the bifurcation parameter before and after the interior crisis occurs, we displayed in Fig. 5, the chaotic signal detected by the photodiode, which is propor-

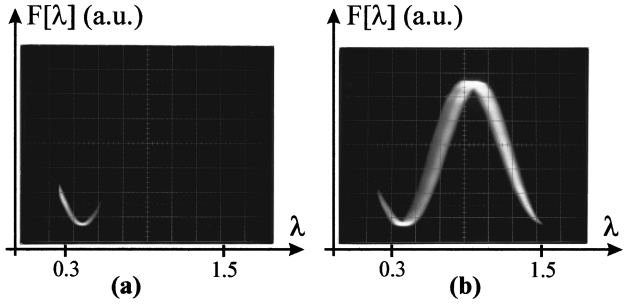

FIG. 5. Experimental visualization of the dynamical regime in the (λ, F) plane observed in the case of Fig. 4(b). In (a), chaotic regime for $\beta_\lambda < \beta_s$; the attractor lies at the bottom of the $\sin^2$ function, in a narrow λ interval. In (b), chaotic regime for $\beta_\lambda > \beta_s$; the unstable orbit lies within a period of the $\sin^2$ function, corresponding to a wide λ interval.

tional to the left member of Eq. (3), as a function of the variable λ. First, in Fig. 5(a), the bifurcation parameter was set at a value $\beta_\lambda = 1.2$ nm, which is slightly less than the critical value β_s. The chaotic region lies at the vicinity of the bottom of the $\sin^2$ curve, within a narrow λ interval [0.25 nm, 0.56 nm]. When increasing β_λ past β_s, the operating region of the F function lies suddenly from the previous valley to the next peak of the $\sin^2$ curve, as shown in Fig. 5(b), which was obtained for $\beta_\lambda = 1.5$ nm ($\beta = 4$). Then, the unstable orbit lies within a much wider λ interval [0.25 nm, 1.5 nm]. These evolutions are the same as the theoretical predictions [similar results that are not reported here, can be obtained with a 7 cm thick calcite slab (OPD = 11 mm and $N = 7$), yielding $\beta = 22$].

IV. CONCLUSION

In summary, we have reported a system in which wavelength-induced nonlinearities are used to generate chaotic fluctuations of the wavelength of a tunable laser diode. The advantage of the device is its high simplicity, flexibility, and applicability as a generator of chaos in which the parameters governing the nonlinearity can be controlled accurately through wavelength. The fact that the nonlinearity is extrinsic to the laser chip is another advantage. It is expected that a wide range of dynamical properties can be obtained, as will be discussed in a longer paper, along with considerations on the Lyapunov exponents and the entropy of chaos. Though the description was limited in these first experiments to routes to chaos produced by $\sin^2$ functions, we emphasize that a variety of nonlinear functions can be used with suitable spectral filters in the feedback loop. This is different from other experimental configurations reported up to the present [1–7,10–12], which are based on intensity or polarization. Physically it is essentially due to the fact that wavelength can be handled and controlled with experimental configurations much simpler than those based on power. This should open the way to systems with complicated nonlinear functions. Moreover, the latter could be synthetized and changed in real time, using electrically tunable spectral filters such as low-voltage integrated electro-optic Solc or Lyot filters [15]. This should allow the realization of ''tunable'' generators of chaos featuring a number of different complex dynamics that could be tuned easily. It should also be mentioned that the dimension of chaos can be very high.

An estimate of the dimension of the chaotic attractor is given by the relationship $0.4\,\beta T/\tau$, which applies to delayed-feedback nonlinear systems [8,16], which are known to be very simple devices producing hyperchaos, i.e., very high dimensional chaos. For the device reported here (with the 7 cm thick calcite plate) this yields a dimension of 5×10^2, which corresponds to approximately 250 zero and positive Lyapunov exponents. Straightforward applications deal with increasing confidentiality in signal encryption for secure communications using high dimensional chaos. We also speculate that chaos in wavelength as defined in this paper might be extended to all optical devices.

ACKNOWLEDGMENT

The support of France Telecom (Contract No. 931B0190) is gratefully acknowledged.

[1] K. Ikeda, H. Daido, and O. Akimoto, Phys. Rev. Lett. **45**, 709 (1980); K. Ikeda and M. Mizuno, IEEE J. Quantum Electron. **21**, 1429 (1985).

[2] F. A. Hopf, D. L. Kaplan, H. M. Gibbs, and R. L. Shoemaker, Phys. Rev. A **25**, 2172 (1982); M. W. Derstine, H. M. Gibbs, F. A. Hopf, and D. L. Kaplan, *ibid.* **27**, 3200 (1983).

[3] J. Y. Gao, J. M. Yuan, and L. M. Narducci, Opt. Commun. **44**, 201 (1983).

[4] R. Vallée and C. Delisle, Phys. Rev. A **31**, 2390 (1985); R. Vallée, C. Delisle, and J. Chrostowski, *ibid.* **30**, 336 (1984).

[5] Y. Liu and J. Ohtsubo, J. Opt. Soc. Am. B **9**, 261 (1992); T. Takizawa, Y. Liu, and J. Ohtsubo, IEEE J. Quantum Electron. **30**, 334 (1994).

[6] P. Glorieux and A. Le Floch, Opt. Commun. **79**, 229 (1990).

[7] Chaotic wavelength fluctuations seemed mostly useless and a state that any laser diode should be avoided from. A review on laser diodes is found in H. Kawaguchi, *Bistabilities and Non Linearities in Laser Diodes* (Artech House, Boston, 1994), Chap. 7.

[8] B. Dorizzi, B. Grammaticos, M. Le Berre, Y. Pomeau, R. Ressayre, and A. Tallet, Phys. Rev. A **35**, 328 (1987).

[9] H. Porte and J. P. Goedgebuer, Opt. Commun. **51**, 331 (1984); J. P. Goedgebuer, M. Li, and H. Porte, IEEE J. Quantum Electron. **23**, 153 (1987).

[10] M. W. Derstine, H. M. Gibbs, F. A. Hopf, and L. D. Sanders, IEEE J. Quantum Electron. **21**, 1419 (1985).

[11] For a recent review, see C. O. Weiss and R. Vilaseca, in *Non Linear Dynamics*, edited by H.-G. Schuster (VCH, New York, 1991); M. Tachikawa, F. Hong, K. Tanii, and T. Shimizu, Phys. Rev. Lett. **60**, 2266 (1988).

[12] L. Fabiny, P. Colet, R. Roy, and D. Lendstra, Phys. Rev. A **47**, 4287 (1993).

[13] See, for example, H. O. Peitgen, H. Jurgens, and D. Saupe, *Chaos and Fractals* (Springer-Verlag, Berlin, 1992), Chap. 11.

[14] S. J. Chang and J. Wright, Phys. Rev. A **23**, 1419 (1981); C. Grebogi and E. Ott, Physica D **7**, 181 (1983).

[15] G. Ramantoko, J. P. Goedgebuer, and H. Porte, Opt. Lett. **21**, 372 (1996); P. Mollier, H. Porte, and J. P. Goedgebuer, Appl. Phys. Lett. **60**, 274 (1992).

[16] M. Le Berre, E. Ressayre, A. Tallet, H. M. Gibbs, D. L. Kaplan, and M. H. Rose, Phys. Rev. A **35**, 4020 (1987).